

Supplementary Materials for

Annexin A1–dependent tethering promotes extracellular vesicle aggregation revealed with single–extracellular vesicle analysis

Maximillian A. Rogers, Fabrizio Buffolo, Florian Schlotter, Samantha K. Atkins, Lang H. Lee, Arda Halu, Mark C. Blaser, Elena Tsolaki, Hideyuki Higashi, Kristin Luther, George Daaboul, Carlijn V.C. Bouten, Simon C. Body, Sasha A. Singh, Sergio Bertazzo, Peter Libby, Masanori Aikawa, Elena Aikawa*

*Corresponding author. Email: eaikawa@bwh.harvard.edu

Published 16 September 2020, *Sci. Adv.* **6**, eabb1244 (2020)
DOI: [10.1126/sciadv.abb1244](https://doi.org/10.1126/sciadv.abb1244)

The PDF file includes:

Figs. S1 to S8
Legend for movie S1
Legend for data file S1

Other Supplementary Material for this manuscript includes the following:

(available at advances.sciencemag.org/cgi/content/full/6/38/eabb1244/DC1)

Movie S1
Data file S1

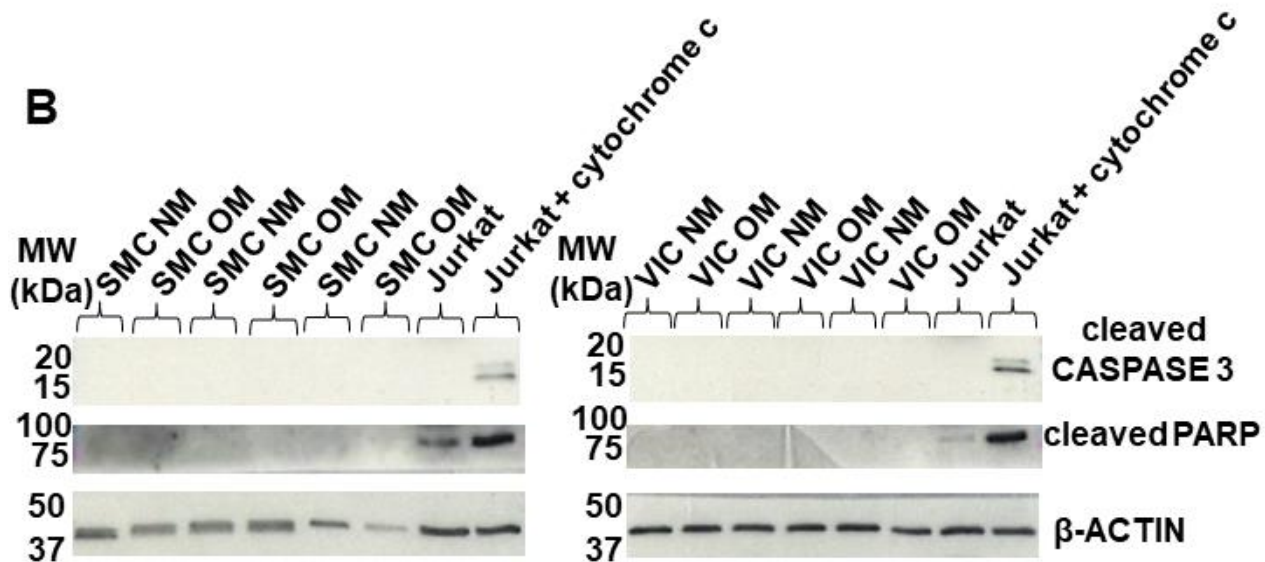
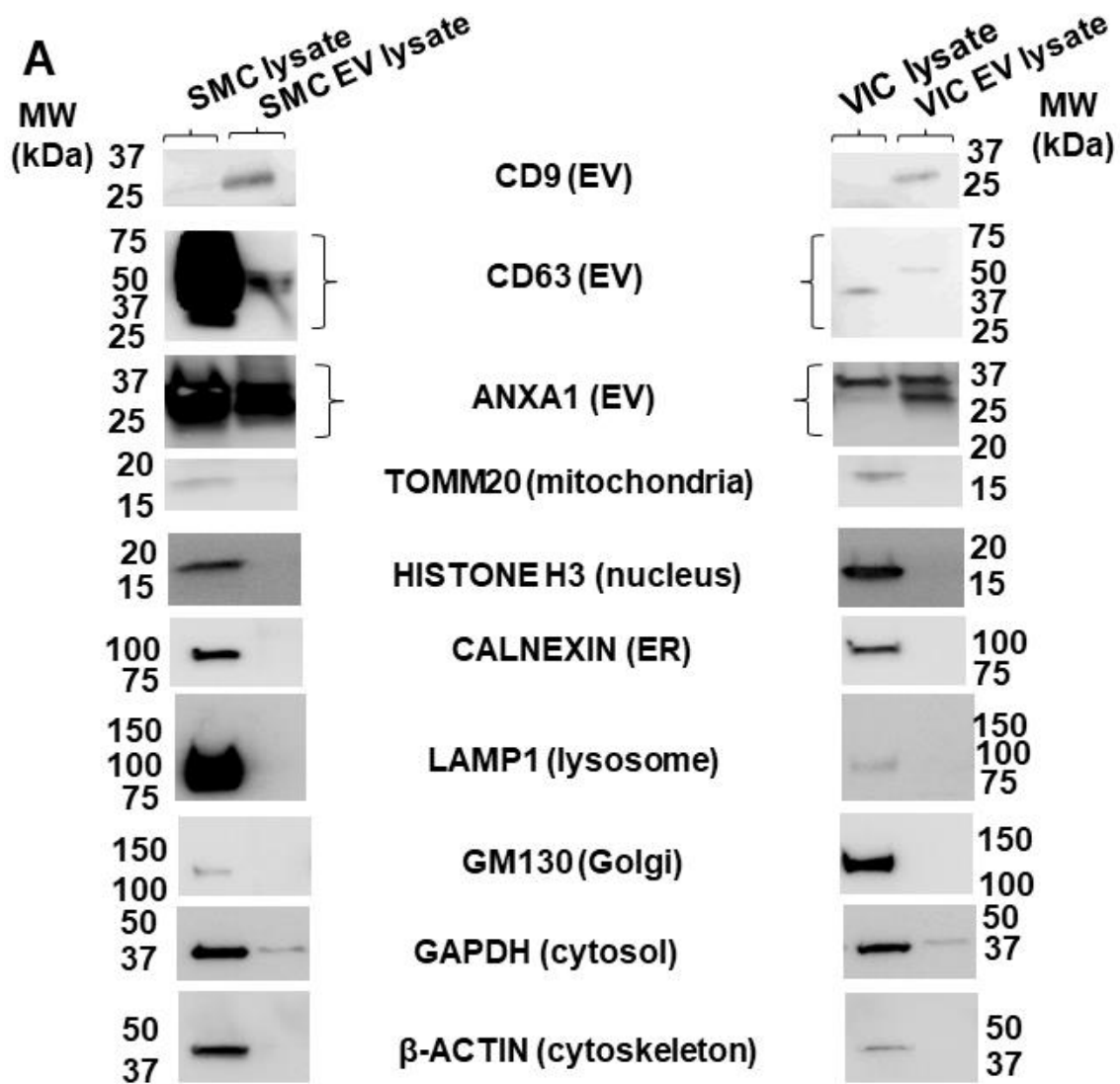


Fig. S1. EV isolation purity indicated by Western blot comparison of EV to whole cell lysate.

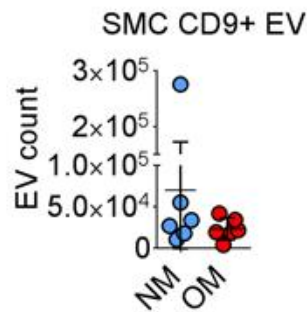
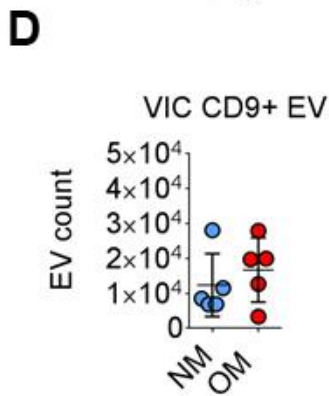
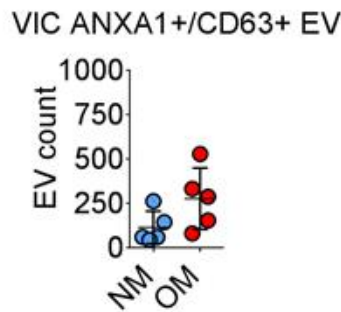
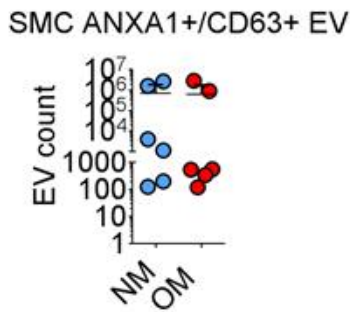
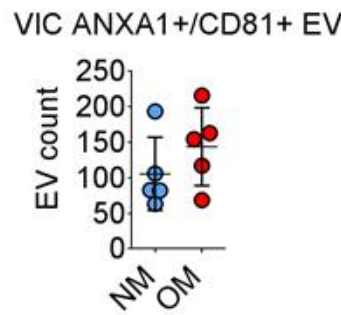
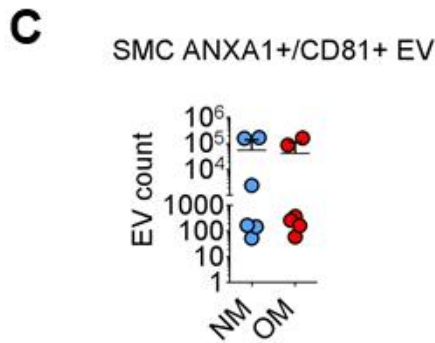
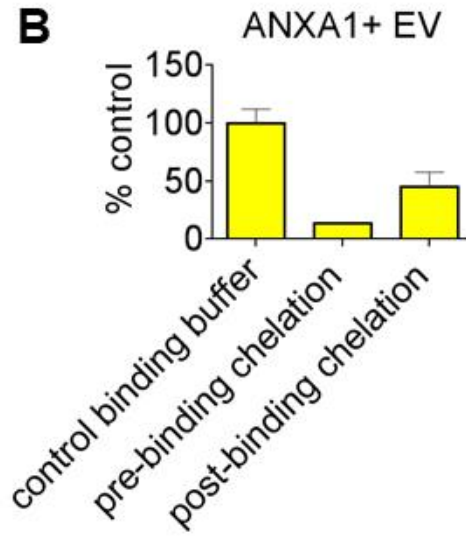
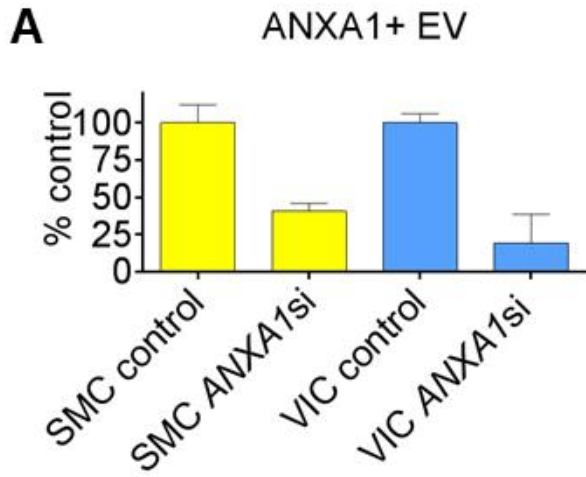
(A) Western blot comparison of EV (CD9, CD63, ANXA1), mitochondria (TOMM20), nucleus (histone H3), endoplasmic reticulum (ER; calnexin), lysosome (LAMP1), Golgi (GM130), cytosol (GAPDH), and cytoskeleton (β -actin) markers in equal loaded (protein content) EV and whole cell SMC and VIC lysates ($N = 3$ donors with one representative blot of three shown). (B) Cleaved caspase 3 (not detected) and cleaved PARP (not detected) Western blots of whole cell lysates for SMC and VIC cultured in NM and OM for two weeks ($N = 3$ donors). Jurkat cell lysates with and without cytochrome c treatment included as antibody positive control.

Fig. S2. Enriched pathways based on significantly changed proteins in OM from SMC EV.

Connections in networks denote common proteins between pathways (more proteins equate to a thicker connection). Node sizes correspond to significance of enrichment (proportional to $-\log(q\text{-value})$); $N = 9$ donors. Shared pathways enriched in both SMC EV and VIC EV in OM indicated by blue nodes on the adjacent network.

Fig. S3. Enriched pathways based on significantly changed proteins in OM from VIC EV.

Connections in networks denote common proteins between pathways (more proteins equate to a thicker connection). Node sizes correspond to significance of enrichment (proportional to $-\log(q\text{-value})$); $N = 7$ donors. Shared pathways enriched in both SMC EV and VIC EV in OM indicated by blue nodes on the adjacent network.



SMC ANXA1+ CD9+ EV

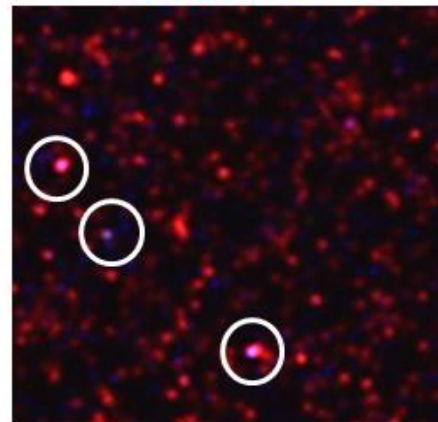
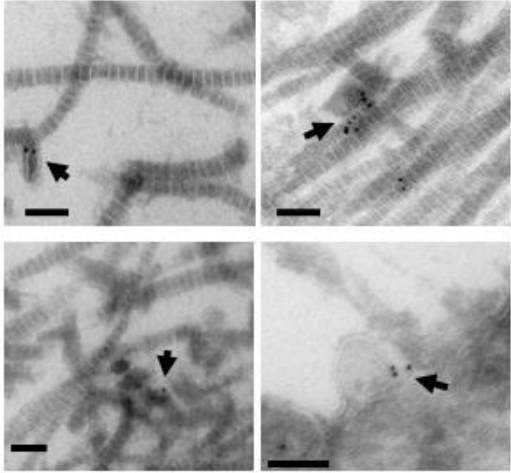


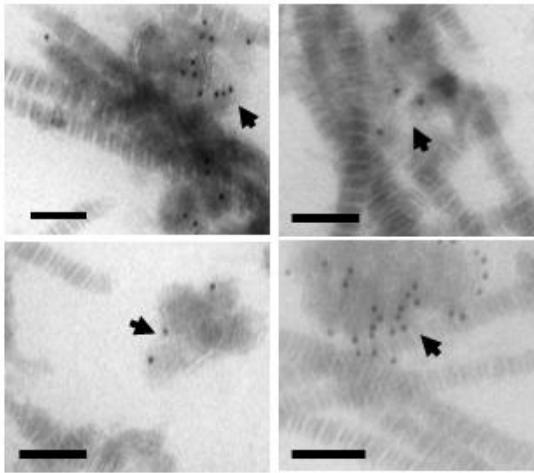
Fig. S4. Single-EV microarray assessment of ANXA1 detection on SMC EV and VIC EV.

(A) SMC and VIC ANXA1+ EV counts presented as percent control for SMC and VIC incubated with *ANXA1* siRNA (*ANXA1*si) or control siRNA ($N = 3$ technical replicates, error bars are mean \pm SD). (B) ANXA1 detection on captured SMC EV with or without calcium chelation incubated pre- and post-EV binding to microarray chips; $N = 3$ technical replicates, error bars are mean \pm SD. (C) SMC ($N = 6$ donors) and VIC ($N = 5$ donors) ANXA1+/CD63+ EV, ANXA1+/CD81+ EV and (D) CD9+ EV in NM and OM; error bars are mean \pm SD. Representative single-EV microarray image for ANXA1+/CD9+ EV (white circles), with quantification of ANXA1+/CD9+ EV included in Fig. 3E.

A Human carotid artery



Human aortic valve



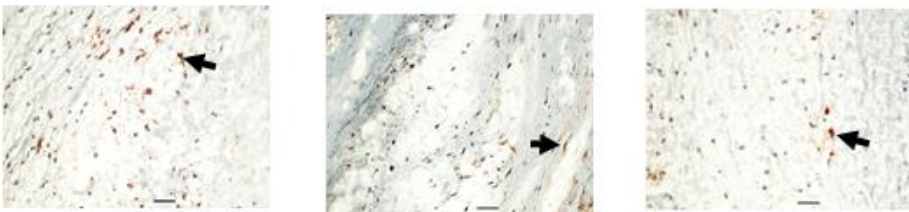
B Non-calcified human carotid artery ANXA1



Calcified human carotid artery ANXA1



Non-calcified human aortic valve leaflet ANXA1



Calcified human aortic valve leaflet ANXA1

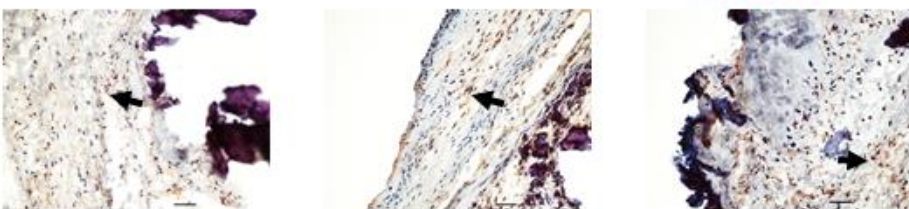


Fig. S5. ANXA1 is on tethered EV in human cardiovascular tissues. (A) Calcified human carotid artery and aortic valve tissue transmission electron microscopy with ANXA1 immunogold labeling (black dots) on tethered EV (arrows) in collagen ECM. Scale bars, 100 nm; $N = 5$ donors, with four representative images shown and an additional image included in Fig. 4A. (B) ANXA1 immunohistochemistry (red color) in non-calcified and calcified (hematoxylin stain, purple color) human carotid artery and aortic valve tissues. Scale bars, 50 μm ; $N = 5$ donors, with 3 donors shown and an additional donor image included in Fig. 4A.

Fig. S6. Annexin mRNA expression and protein total abundance is largely not altered in calcified human tissues and cells. (A) Unlabeled proteomics analysis of annexins A1, A2, A5, A6, and S100A11 in non-calcified and calcified human aortic valve tissue; $N = 9$ donors, with S100A11 detected in 8/9 non-calcified and 7/9 calcified donor tissues, ANXA1 detected in 9/9 donors, ANXA2 detected in 9/9 donors, ANXA5 detected in 9/9 donors, and ANXA6 detected in 5/9 non-calcified and 1/9 calcified donor tissues; error bars are mean \pm SD, analyzed by Welch's t-test. (B) mRNA levels of annexins A1, A2, A5, A6 in non-calcified and calcified human carotid artery and aortic valve tissues; analyzed by Welch's t-test, $N = 5$ donors, mean \pm SD. (C) Human SMC and VIC mRNA levels of annexins A1, A2, A5, A6 in NM or OM incubated with control siRNA (control) or ANXA1 siRNA (ANXA1si) for two weeks; error bars are mean \pm SD from 3 donors, analyzed by ANOVA, *** $P < 0.001$, ** $P < 0.01$, * $P < 0.05$.

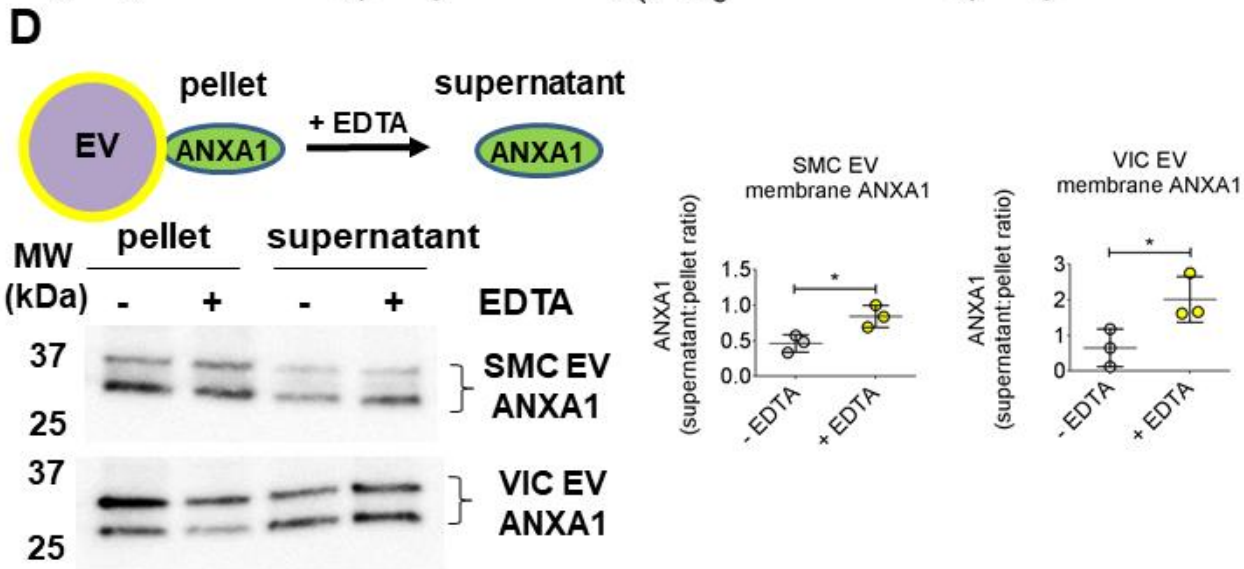
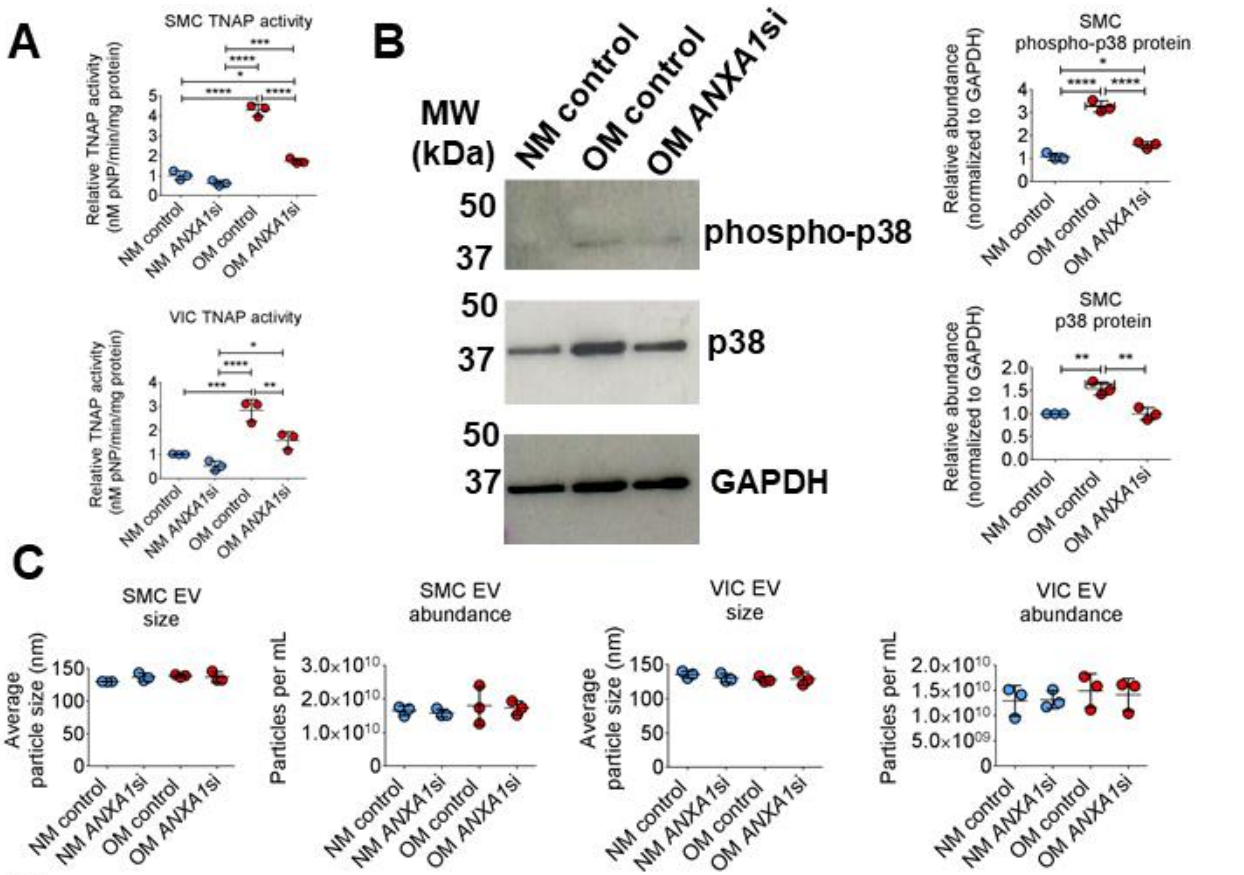


Fig. S7. ANXA1 is on the surface of SMC and VIC EV. (A) TNAP activity in human SMC and VIC in NM or OM incubated with control siRNA (control) or *ANXA1* siRNA (*ANXA1*si) for two weeks. Error bars are mean \pm SD from 3 donors; analyzed by ANOVA. (B) Total p38 and phospho-p38 protein in SMC cultured in NM or OM with control or *ANXA1*si for two weeks. Error bars are mean \pm SD from 3 donors; analyzed by ANOVA. (C) Human SMC EV and VIC EV size and quantity in conditioned media from cells cultured in NM or OM with control or *ANXA1*si; $N = 3$ donors, error bars are mean \pm SD. (E) Illustration showing experiment design to confirm EV surface localization of ANXA1. ANXA1 Western blots from human SMC EV and VIC EV incubated with EDTA to release ANXA1 from the EV surface into the supernatant; quantification is the sum of both bands, $N = 3$ donors, error bars are mean \pm SD, analyzed by Welch's t-test. **** $P < 0.0001$, *** $P < 0.001$, ** $P < 0.01$, * $P < 0.05$.

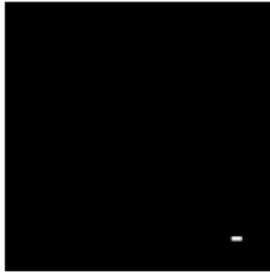
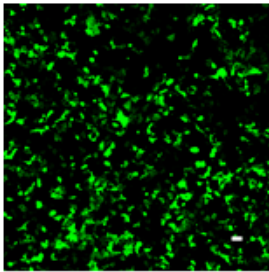
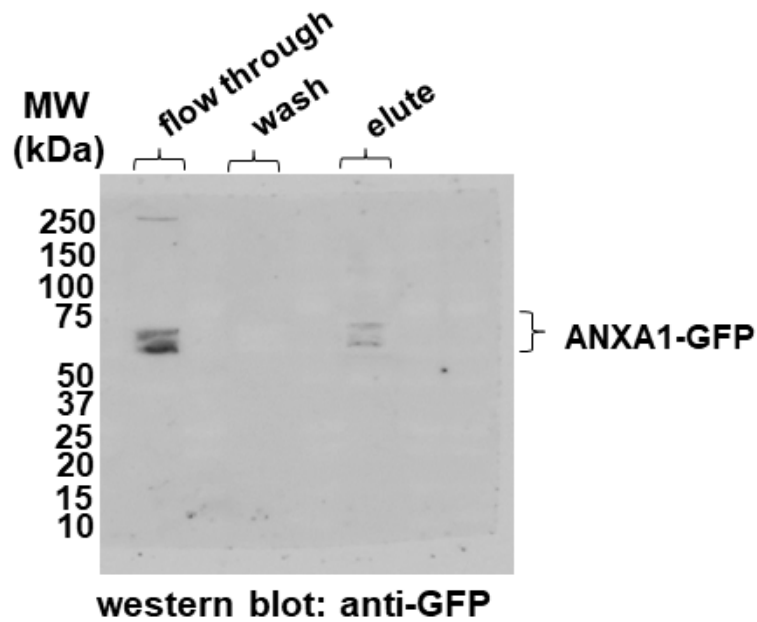
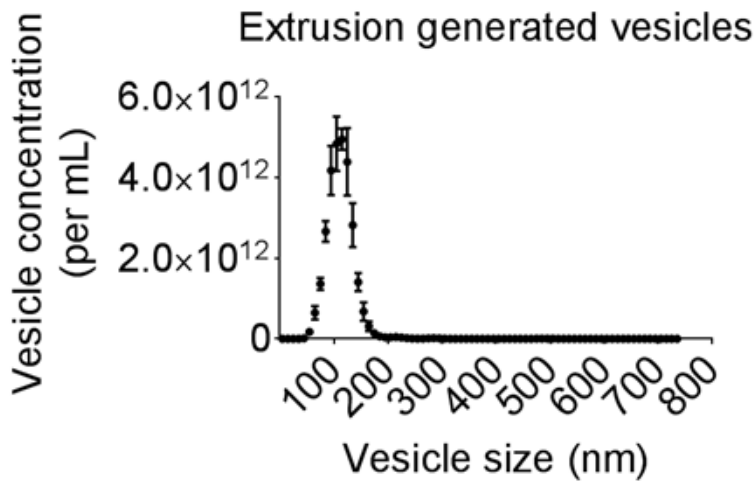
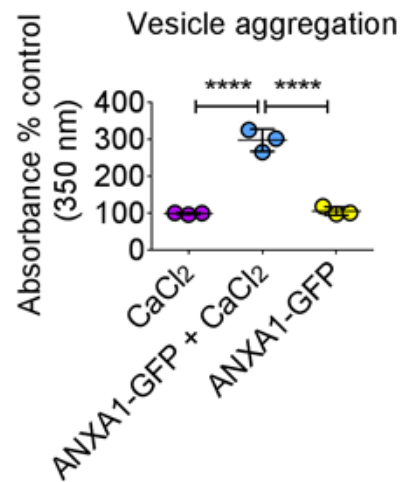
AHEK-293 cells
(no transfection)HEK-293 cells
(ANXA1-GFP transfection)ANXA1 immunoprecipitation**B****C**

Fig. S8. Immunopurification of ANXA1-GFP protein and extrusion generated vesicles nanoparticle tracking analysis. (A) Live cell confocal microscopy of HEK-293 cells transfected with human ANXA1-GFP tagged plasmid; scale bars, 50 μm . Immunoprecipitation Western blot of eluted ANXA1-GFP protein used for confocal imaging of ANXA1 binding to polyvinyl alcohol swelling generated phosphatidylserine vesicles. (B) Nanoparticle tracking analysis of filter extrusion generated phosphatidylserine vesicles size; error bars are mean \pm SD from 5 replicate measurements. (C) Extrusion generated phosphatidylserine vesicle aggregation in buffer containing 1 mmol/L CaCl_2 with 0 μg ANXA1-GFP (CaCl_2) or 1 μg ANXA1-GFP (ANXA1-GFP + CaCl_2), or 1 μg ANXA1-GFP in buffer without CaCl_2 (ANXA1-GFP). Error bars are mean \pm SD from 3 experimental replicates; analyzed by ANOVA, **** $P < 0.0001$.

Movie S1. ANXA1 tethered vesicles. Confocal Z stack video of phosphatidylserine swelling generated vesicles (purple color) incubated with human green fluorescent protein tagged ANXA1 (green color). Width: 32.46 μm , height: 32.46 μm , depth: 18.90 μm . Corresponding image also included in Fig. 5A.

Dataset S1. Proteomics and network analysis. Human SMC EV ($N = 9$ donors) and VIC EV ($N = 7$ donors) proteomics datasets, statistical analysis, comparative analysis, and pathway network analysis.